Vol. 205, No. 1, 1994 BIOCHEMICAL AND BIOPHYSICAL RESEARCH COMMUNICATIONS
November 30, 1994 Pages 638-644

In vivo IMAGING OF THE INTERIOR OF *Tradescantia zebrina* LEAVES BY OPTICAL CROSS-CORRELATION INTERFEROMETRY

Li Ning[1], Zhao Lu[2], Larry S. Daley[1]* and J. B. Callis[2]

[1] Dept. of Horticulture, ALS 4017, Oregon State University, Corvallis, OR 97331

[2]Dept. of Chemistry, University of Washington, Seattle, WA 98195

Received October 11, 1994

Summary: Using optical correlation interferometry, a novel method for plant sciences, we in imaged *in vivo* the z-direction, perpendicular to the leaf surface, through *Tradescantia zebrina* leaves. Non-invasively we determined number of major cell layers, followed the time sequence of decrease in cell z-axis after exposure of tissues to high salt, and observed disruption of cells caused by freezing and thawing.

We seek non-invasive measurement inside plant leaves. Our ultimate objective is to study the biochemistry of plants *in vivo* in three dimensions (3-D) by UV, visible and near infrared spectroscopy. Since Coblenz (1) to recent times (2-8) *in situ* plant leaf spectra, has been done in quasi one dimensional form (1-D) with the x-y plane perpendicular to the light source axis plus the z-axis, depth axis, collapsed into one point. Since the 1-D approach cannot resolve patterns of structures across the lamina of the leaf which have applied and theoretical significance we developed a two (2-D) dimensional (x-y image) spectrophotometer (9,10). 2-D images have great utility; however z-axis spectra is also important because leaf cell biochemistry is most frequently specialized in tissues perpendicular to this axis. Thus, complete optical characterization of leaves requires z-direction data.

Low-coherence reflectometry is used by some medical scientists (11-13), but novel to plant sciences. *Tradescantia* has large, well defined cells, where Robert Brown (1828) first observed protoplasmic streaming (14). *Tradescantia zebrina*, has leaves well suited to this method, since its leaves have few leaf cell layers, regularly formed and distinct, that vary in number between the silver and green bands that extend along the length of the leaf (described below).

Many approaches are available to image along the z-axis as well as the conventional x and y axes. To mechanically slice the sample into sections perpendicular to the z-axis is destructive and thus, reveals data from only one instant in time for each set of tissue slices. This, because of biological variability

*Author to whom correspondence should be directed.
FAX:(503) 737-3479; e-mail: daleyl@ava.bcc.orst.edu.

0006-291X/94 $5.00

between tissue samples, introduces unwanted variables into the composite time sequences generated from the pooled samples. In optical tomography (*e.g.* 15), the straight forward use of parallel sheets of light becomes problematic for small objects. Therefore, using a microscope, one captures a series of optical slices by simple varying the focal distance; then one corrects the images for above and below plane out of focus contributions (16). The resulting stack of 2-D images can then be rendered into 3-D images using the same techniques that MRI (17) uses to make 3-D images.

One can get z-axis data by tracing photon flow through samples. A way to do this is to give a pulse of light and time photon arrival. This requires super fast electronics to measure small objects, *i.e.* to resolve one micron requires $4x10^{-15}$ s timing. Light pulses of a duration this short require very expensive, and not easily portable, laser technology (*e.g.* 18).

There is an alternative way: non-monochromatic light undergoes random fluctuations on a time scale set by the inverse bandwidth of the light source (19). These fluctuations can be characterized by their correlation time τ given by the equation:

$$\tau=\lambda^2*(\pi\Delta\lambda*c)^{-1}$$

Here λ is wavelength, * indicates multiplication, and c is the speed of light, which in a vacuum is $2.998*10^8$ meters per second, approximated here as $3*10^8$ $m*s^{-1}$. Thus, for a center wavelength of 450 nm, and a band with of 90 nm, $\Delta\lambda$=90 nm; we can approximate: τ as $(450\ nm)^2/(\pi*90\ nm*3*10^8\ m*s^{-1})$ $=2.38*10^{-15}$ s, which is enough time resolution for a spatial resolution of better than a micron.

A fluctuating light source can replace pulse light as the probe. From linear systems theory (*e.g.* 20), it can be shown that one can do the equivalent to an impulse response experiment, by cross correlating the random probe beam with the output beam. It is not yet possible to perform the cross correlation in the time domain because detectors of sufficiently wide bandwidth and means to record the waveforms do not exist. Instead we use the spatial domain with a Michelson interferometer (19) as an analog computer of the cross correlation function. Such a device is available commercially (Precision Reflectance Interferometer, Model 8504A, Hewlett-Packard Co, Palo Alto, CA) implemented in a convenient fiber optic form. This device, developed to test fiber optic instrumentation, can profile human skin in depth (13).

The sample is placed at the end of the interferometer, and replaces the usual mirror. In this case, the light will strongly constructively interfere whenever, the path lengths of the moving reference mirror and a reflecting surface in the test object are equal. This matching condition, known as the center burst, appears as a spike ("peak") in the waveform (interferogram) of intensity vs position of the reference arm. One therefore obtains a series of peaks each corresponding to a specific reflecting surface of the object. And, as the photons transverse a highly scattering medium, back scattering of light exhibits an exponential decay in space, corresponding to the exponentially declining probability that the photons penetrate a specific distance without being scattered.

Materials and Methods

Materials and leaf manipulations. Zebrina (*Tradescantia zebrina* Bosse, Commelinaceae), grown in a Univ. of Washington, Seattle, Botany Dept. greenhouse was picked in late August and September. Poly-

styrene spheres (Polysciences Inc., Warrington, PA) diameters were 0.2 microns (μm). To test the effects of hypertonicity the leaf slivers were bathed in appropriate solutions during assay. To test cell integrity conductivity measurements were taken with a standard multimeter, with the electrodes separated by 1.2 mm, then calibrated relative to NaCl solutions. Freezing experiments were done while samples were in the instrument by holding a chip of dry ice to the slide that supports the cuvette. Before and during freezing, and after thawing measurements were taken without moving the sample. Verification of freeze damage was done in parallel experiments, as is standard, by conductivity measurements. Multiple replications of experiments were done to assure reproducibility of cross correlation data.

Instrumentation. The light microscope used was a Nikon Microphot-FXA obtained from Meridian Instrument Co, Inc. (Kent, WA). A 91.4 micron diameter wire was used to calibrate tissue width. A newly constructed imaging fluorometer (Ning, *et al.*, unpublished) was used to image fluorescence yield. The optical autocorrelation interferometer (Precision Reflectance Interferometer, Model 8504A, Hewlett-Packard Co, Palo Alto, CA) was operated at 1300 nm (21-23) illuminating the leaf from the lower surface. Data was signal averaged by instrument, and processed using MATLAB (The Math-Works, Natick, MA), Statgraphics Plus (Manugistics Inc., Rockville, MD) and PhotoFinish (Softkey International Corp., Marietta, GA).

Results and Discussion

To test of the optical autocorrelative interferometer and illustrate the nature of the cross correlation functions we made a cuvette as shown in upper part of Fig. 1. Below this in Fig. 1, three sets of traces show the peaks in the cross correlation function numbered to correspond to the numbered surfaces of the cuvette. The peaks labeled with numbers without primed superscripts define the object and its dimensions, if one knows the index of refraction of the cuvette materials. The peaks labeled with numbers with primed superscripts represent multiple secondary reflections within the object. The top trace shows the cross correlation function obtained with air in the cuvette. The middle trace shows the cross correlation function after the cuvette has been filled with water. Now the secondary reflections are suppressed due to decrease reflectivity at glass water boundary compared to the glass air boundaries of the previous trace. The distance between peaks 2 and 3 is greater, because light travels more slowly in water than air. The lowest set of traces is from a cuvette filled with a water suspension of polystyrene microspheres; here the length scale has been expanded to show the data more clearly. In these traces, photon density declines exponentially as light transverses this scattering medium. The second, longer, trace in this part of the figure was generated using a cuvette in which the cavity dimensions have been expanded as indicated by the shift of peak 3 to peak 3; here the decline in light follows the same exponential form, but over a longer distance.

Light micrographs show the structural differences in the transverse sections of silver and green tissues of *T. zebrina*.(Fig. 2 left and right respectively); above the micrographs are the corresponding cross correlation images. Note the greater width of the middle layer of tissue that contains the bulk of the photosynthetic apparatus, and the doubling of upper cell layers in the green, as opposed to the silver, sections of the leaf. Notice how the cross correlation images correspond to the different structures found in these leaves. Since we get the same cross correlation images in intact leaves (not shown) it is apparent we can determine cell layers non-invasively. Fluorescence activity measurements (not shown) demonstrated that the green section is photosynthetically active and the low chlorophyll (silver) section is almost inactive.

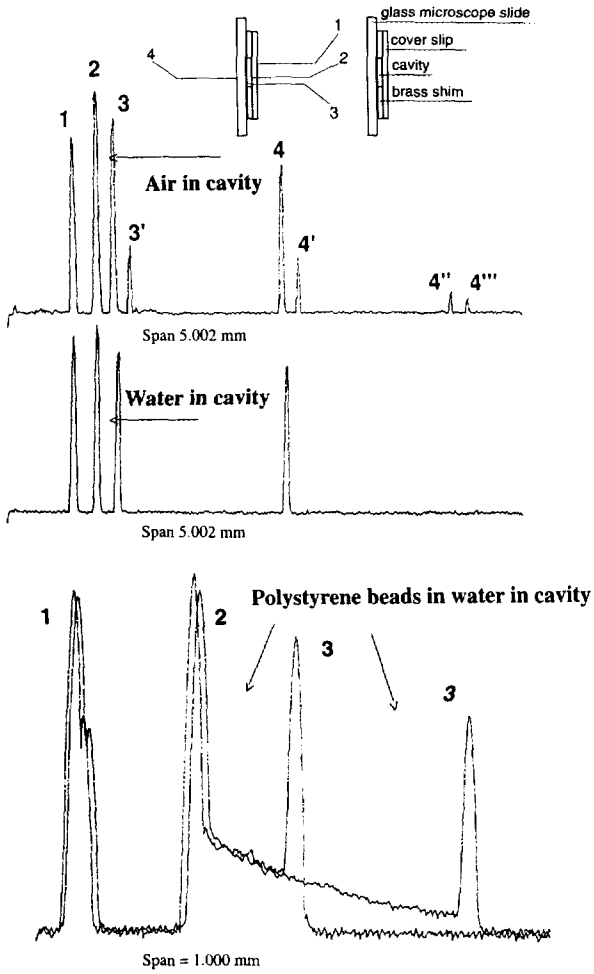

Figure 1. Optical cross correlation interferometer response in model system. The model is diagramed in upper left of figure; a second diagram of the model, upper middle of the figure, shows the numbered locations of the reflection sites which correspond to peaks in the data traces; secondary reflections are indicated by numbers with superscripts ', '', and '''. The three examples of data traces from the instrument are immediately below the diagrams of the model. The spans of the traces are indicated on x-axes. The cavities are located between peaks 2 and 3. The uppermost, middle and lowest traces correspond, respectively, to cavities filled with air, water and a suspension of 0.2-μm polystyrene spheres in water. The lowest set of traces illustrates data from two scans, with the second scan derived from analysis of a model with a longer cell length. The longer cell length displaces peak 3 to peak 3. Notice that the replacement of air by water removes the secondary reflections and also increases the apparent distance between peak 2 and peak 3, due to the increase in time that light takes to pass through water, about 1.33 x the time in air.

Figure 3 shows a time sequence of effects of hypertonic solutions on cross correlation images. The data shown is for silver tissue and is presented in the MATLAB image function format which generates a histogram illustrating depth change with time. The darkest lines represent the most intense reflections, and

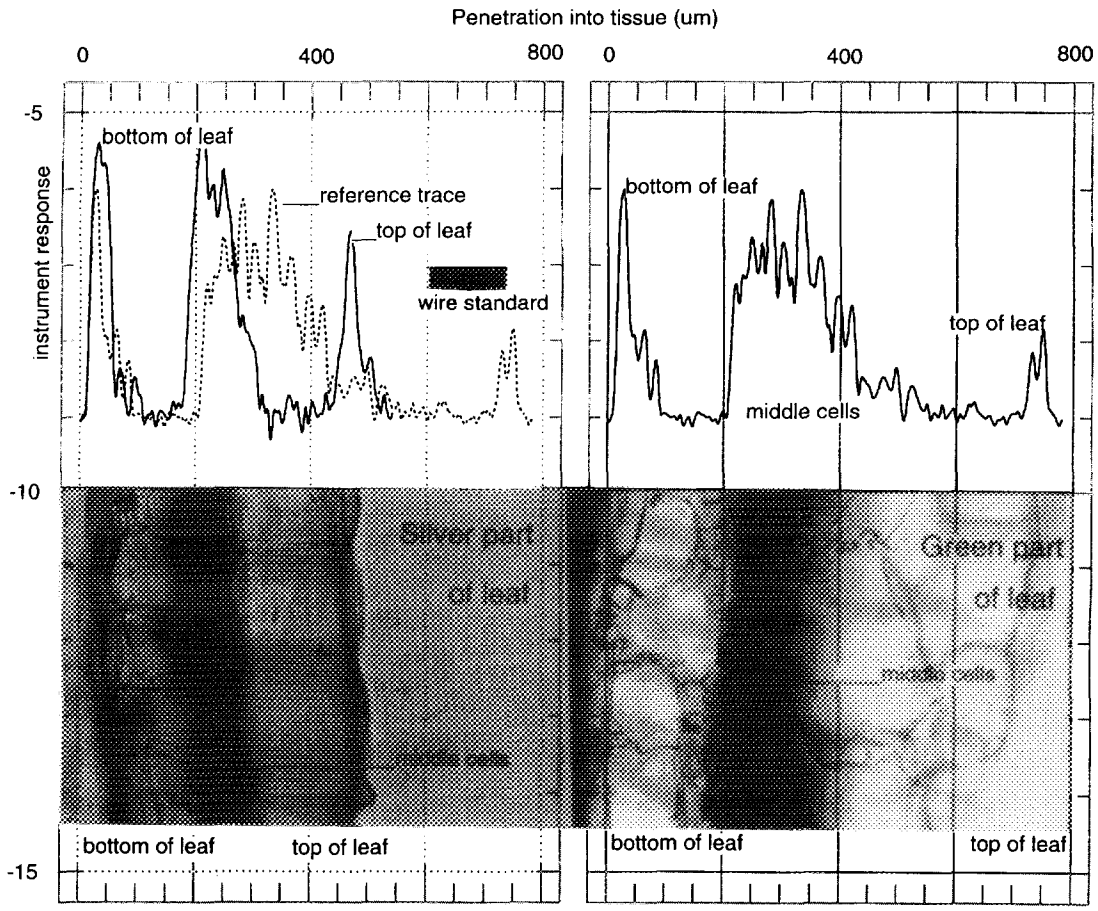

Figure 2. Optical image fit to optical cross-correlation interferometer response of Tradescantia zebrina leaves. This plant has well-marked low chlorophyll 'silver' bands (left in figure), that extend parallel to the central vein in the direction we have assigned as y. These silver bands are separated by high chlorophyll 'green' areas which have one additional upper layer of large cells (right in figure). Leaf width is assigned to the x-direction, leaf thickness, showing different layers of cells is the z-axis. Left figure shows light micrograph of leaf x-z plane showing a cross-section of a silver band; the corresponding optical cross-correlation interferometer trace is superimposed. The right figure shows a light micrograph of leaf x-z plane showing a cross section of a green area, with the corresponding optical cross-correlation interferometer trace. In this micrograph, cell walls not in the plane of the image appear blurred. The wire standard (and the liquid portions of the cells in the traces) appear to be larger on interferometry scale because there is no correction (x 1.33) for the change of the speed of light in aqueous solutions.

correspond to peaks in Figs. 2 and 4, and thus separate the leaf depth profile into upper cells, middle layer cell, and lower cell regions. The upper unlabeled space which increases sequentially, with time, from left to right is free liquid solution above the upper layer of cells, and can be used to indicate the total loss of leaf depth. The time sequences are separated by the sequential abrupt changes in cell depth, which are referenced to lowest part of lower cells. Since the experimental variable is external high salt which takes water out of the cells, and we know that these changes require immersion high salt solutions, it is most logical to

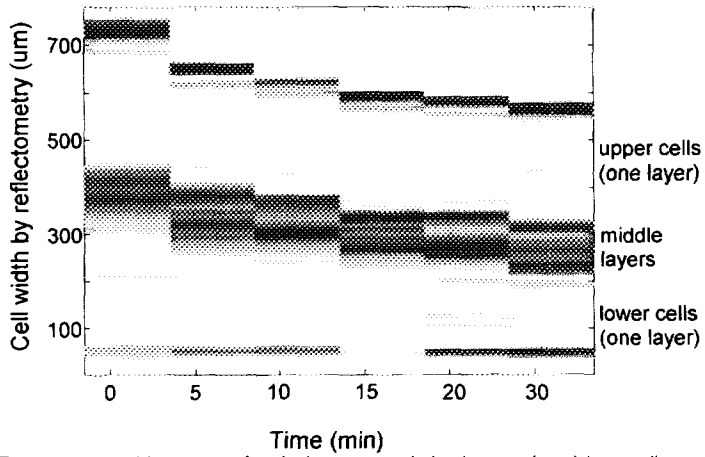

Figure 3. Time sequence histrogram of optical cross-correlation images (z-axis) as a silver section of the leaf immersed in 15% sodium chloride solution. The plot was prepared using Mat-lab image function and PhotoFinish.

assume that depth loss is a function of loss of cell water. Thus we can determine that lower cells lose water more readily than upper cells, and middle cells resist dehydration. We expect this technology to be useful in our *in vivo* spectroscopic drought stress investigations.

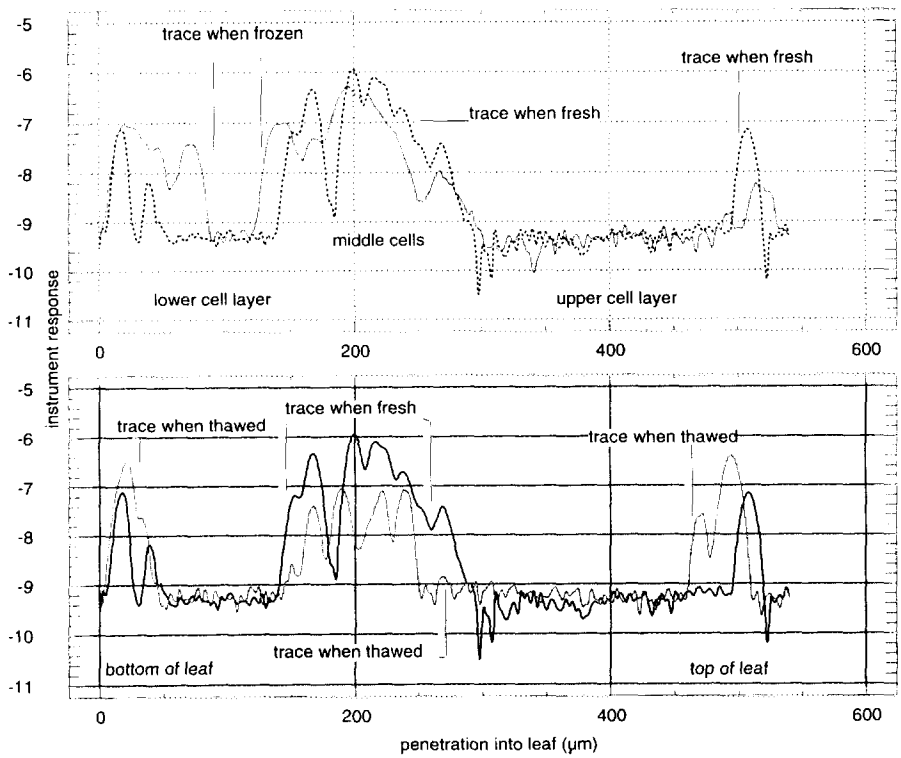

Figure 4. Optical cross-correlation images (z-axis) of a silver section of the leaf before and after freezing and then when thawed. The upper figure compares traces when fresh and frozen; the lower figure compares the fresh and thawed traces. The traces were prepared using Stagraphics Plus Q-spline plot.

Figure 4 shows optical cross correlation images of silver tissue describing the effects of freezing leaf tissue on cell z-axis. The upper part of the figure shows tissue before freezing and when frozen, notice the increase in reflectance of the lower layer of cells where the light enters, and the decrease in light reaching the upper part of the leaf. The lower part of the figure compares the fresh tissue signals with signals after thawing, illustrating the effects of mechanical damage on the middle cell layers. The increase in reflectance from the upper part of the leaf indicates that the disruption of the middle layer has allowed more light to reach the lower cells. In this process the conductivity of the external solution increased significantly as a result of spilling cell contents of thaw ruptured cells into surrounding solution. It may be possible to use this technology to determine freeze damage in the field, a matter of some importance to the important plant nursery industry of Oregon.

Acknowledgments

This work was supported by a grant from the Herman Frasch Foundation (332-HF92). We are grateful to Lloyd Burgess, Paul Shelly and Ines Ferreira of the Center for Process Analytical Chemistry (Chemistry Dept., Univ. of Washington, Seattle) for the loan of the instrument and instruction in its use. The instrument, a Precision Reflectance Interferometer (Model 8504A),was a generous gift from Hewlett-Packard Co (Palo Alto, CA). Stan Gartler (Medical School, Univ. of Washington, Seattle) provided instruction and use of the light microscope. We thank Douglas Ewing (Botany Dept., Univ. of Washington, Seattle) who grew and helped select the experimental plant material, Gerald E. Edwards (Botany Dept., Washington State University, Pullman) for kind advice, and Natalie S. Daley for model diagrams. This paper is Oregon Agricultural Experiment Station Technical paper 10588.

References

1. Coblenz, W.W. (1913). *Bulletin of the Bureau Standards*, **9**, 283-325.
2. Shull, C.A. (1929). *Bot. Gaz.*, **87**, 583-607.
3. Seybold, A. (1933). *Planta*, **18**, 479-508.
4. Rabideau, G.S., French, C.S. and Holt, A.S. (1946). *Amer. J. Bot.*, **33**, 769-777.
5. Butler, W.L. (1972). *Methods in Enzymology*, **24(B)**, 3-25.
6. Ruhle, W. and Wild, A. (1979). *Planta*, **146**, 551-557.
7. Daley, L.S. (1986). *Scientia Hort.* **28**, 165-176.
8. Daley, L.S. (1990). *Plant Physiol. Biochem.*, **28**, 271-282.
9. Ning, L., Ozanich, R., Daley, L.S. and Callis, J. B. (1994). *Spectroscopy*, **97**, 41-48.
10. Ning, L., Danielson, J.D.S., Chozinski, A., Buban, T., Azarenko, A.N., Daley, L.S., Callis, J.B., and Strobel, G.A. (1995). *Scientia Hort.* (Submitted).
11. Huang, D., Swanson, E.A., Lin C.P., Schumann, J.S., Stinson, W.G., Chang, W., Hee, M.R., Flotte, T., Gregory K., Puliafito, C.A. and Fujimoto J.G. (1991). Optical coherence tomography. *Science* **254**, 1178-1181.
12. Hitzenberger, C.K. (1992). *Applied Optics*, **31**, 6637-6642.
13. Schmitt, J.M., Knuttell, A and Bonner R.F. (1993). *Applied Optics*, **32**, 6032-6042.
14. Mabberley, D.J. (1987). *The plant book*, Cambridge Univ. Press, Cambridge, England.
15. Burns, D. H. (1994). *Appl. Spectrosc.* **48(5)**, 12A-19A.
16. Castleman, K.R. (1979). Digital image processing, Prentice-Hall, Inc, Englewood Cliffs, NJ.
17. Treado, P.J., I.W. Levin and E.N. Lewis. (1994). *Appl. Spectrosc.* **48(5)**, 607-615.
18. Savikhin, S., Zhu, Y., Lin, S., Blankenship, R.E. and Struve, W.S. (1994). *J. Phys. Chem.* (in press).
19. Chamberlain, J. (1979). The principals of interferometric spectroscopy, John Wiley, New York, NY.
20. Yu, F.T.S. (1973). *Introduction to diffraction, information processing and holography*, MIT Press, Cambridge, MA.
21. Beck, P.A. (1993). *Hewlett-Packard J.* **1993 (February)**, 49-51.
22. Chou, H. and Sorin W.V. (1993). *Hewlett-Packard J.* **1993 (February)**, 52-59.
23. Booster, D.H., Chou, H., Hart, M.G., Mifsud, S.J. and Rawson, R.F. (1993). *Hewlett-Packard J.* **1993 (February)**, 39-48.